ELSEVIER

Journal of Structural Geology 26 (2004) 287–305

JOURNAL OF STRUCTURAL GEOLOGY

www.elsevier.com/locate/jsg

The interpretation of $^{40}Ar/^{39}Ar$ apparent age spectra produced by mixing: application of the method of asymptotes and limits

M.A. Forster*, G.S. Lister

Structure/Tectonics Group, Research School of Earth Sciences, The Australian National University, Canberra 2601, Australia

Received 14 April 2002; received in revised form 27 July 2003; accepted 17 October 2003

Abstract

A method is presented for the analysis and interpretation of apparent age spectra produced during $^{40}Ar/^{39}Ar$ step-heating experiments. Application of this method is particularly relevant to complex apparent age spectra produced from minerals taken from exhumed metamorphic tectonites, particularly when these rocks once resided in an ancient Argon Partial Retention Zone. Such rocks may have been subject to localised deformation and/or recrystallisation during orogenesis. Yet microstructures relict of earlier episodes of deformation and/or metamorphism may retain relatively old apparent ages. As a result complex apparent age spectra can be produced during a conventional step-heating experiment, and these age spectra often cannot be simply interpreted. The recognition (and the interpretation) of a plateau in such spectra is sometimes uncertain, and in any case, the definition of a 'plateau' is then a concept of limited theoretical validity. To avoid these difficulties an alternative strategy is presented, based on a theory of mixing gas from different microstructural/microchemical reservoirs. This method relies on the definition of asymptotes and limits in sequences of apparent ages in apparent age spectra obtained from step-heating experiments. Frequently measured ages (FMAs) in individual datasets can then be recognized using statistical analysis. The significance of FMAs must be independently assessed.

Keywords: $^{40}Ar/^{39}Ar$ geochronology; Apparent age spectra; Excess argon; White mica; Diffusion domains; Deformation ages

1. Introduction

Determining an age from $^{40}Ar/^{39}Ar$ step-heating experiments has traditionally been undertaken using the 'plateau' method (Dalrymple and Lanphere, 1974). This method is best applied to what are termed 'undisturbed' spectra, where an age is defined from a sequence of concordant steps that record a similar age (McDougall and Harrison, 1999). The scatter of ages between the concordant steps must define the plateau with a $>95\%$ confidence level, for a pre-defined minimum proportion of the total ^{39}Ar release. There is no uniform convention used to define a plateau, although many researchers have suggested criteria that may best define this method (e.g. Fleck et al., 1977; Berger and York, 1981; Foland et al., 1986; Snee et al., 1988; Dallmeyer and Lecorche, 1990). These methods have in common that once a plateau has been defined (using whatever criteria) the age is generally calculated as the error-weighted mean of the steps comprising the plateau.

It is also possible to infer distinctive characteristics of the gas reservoirs in a microstructure, based on the pattern of gas release during a step heating experiment in combination with the sequence of apparent ages recorded in the apparent age spectrum. For example the effects of grain size distribution can be recognized (e.g. Turner et al., 1966; Gillespie et al., 1982; Zeitler, 1987; Lovera et al., 1989), and/or the effects of variation in gradients representing partial loss of radiogenic argon (Turner, 1968). These features determine the 'shape' of an apparent age spectrum, which can be quite complex, but nevertheless readily interpreted in terms of the effects of specific phenomena. However, other effects can also influence the shape of an apparent age spectrum, including excess argon (e.g. Lanphere and Dalrymple, 1971; 1976; Pankhurst et al., 1973; Dalrymple et al., 1975), and recoil (e.g. Horn et al., 1975; Huneke and Smith, 1976; Fergusson and Phillips, 2001). The effects of mixing between different gas reservoirs has been explicitly addressed by Wang et al.

* Corresponding author. Tel.: +61-2-6125-3412; fax: +61-2-6125-3683.
E-mail address: marnie.forster@anu.edu.au (M.A. Forster).

0191-8141/$ - see front matter © 2004 Elsevier Ltd. All rights reserved.
doi:10.1016/j.jsg.2003.10.004

(1980), Harrison and Wang (1981), Gillespie et al. (1982) and Wijbrans and McDougall (1986, 1988).

At this stage in the development of $^{40}Ar/^{39}Ar$ geochronology, the 'plateau' method is used almost universally to interpret the significance of even complex apparent age spectra. Yet there are many apparent age spectra to which the method cannot be rigorously applied, e.g. where a plateau *sensu stricto* does not exist or is not clearly definable (e.g. Foster et al., 1998). These circumstances often arise in 'disturbed' age spectra or spectra that reflect gas release from multiple reservoirs. In these cases it is not suitable and perhaps even incorrect to use the 'plateau' method to define an age. This difficulty led us to a reexamination of theoretical aspects, and thence to a practical numerical method that allows an alternative approach to the interpretation of complex apparent age spectra.

The alternative method is based on the concept that asymptotically converging sequences and/or limits can be recognized in apparent age spectra produced during sufficiently detailed step-heating experiments. The method particularly lends itself to samples where different elements of the microstructure yield distinctly different apparent ages. Microstructural and/or microchemical variation may define distinctive gas reservoirs that potentially can be tapped sequentially during a carefully designed step-heating experiment.

2. Asymptotes and limits in simulated age spectra

Theoretical simulations of the development of apparent age spectra often exhibit the phenomenon of a sequence of ages that asymptotically approaches a limit. For example Fig. 1 illustrates patterns of gas release during simulation of simple diffusion experiments using the *MacArgon* program (Lister and Baldwin, 1996). A model phengite grown at 60 Ma is rapidly cooled below its closure temperature. Millions of years later the model phengite is subjected to a sequence of thermal spikes (Fig. 1a and b). The timing of the individual spikes is in part reflected by the asymptotes and limits that can be determined from these (artificially produced) apparent age spectra.

Each of the apparent age spectra shown in Fig. 1c represents individual temperature–time histories, but these histories vary in the maximum temperature reached during the second thermal pulse. In one case the temperature rises first to 450 °C, but during the second spike, the temperature rises only to 400 °C. In the other case the temperature during the second thermal spike rises to 500 °C. Both thermal spikes involved temperatures well above the notional 'closure temperature' but since the duration of the transient pulse in temperature was relatively short (with a thermal decay constant of 0.1 Ma), complete degassing did not occur. The role of diffusion cannot be dismissed based on simple (and largely incorrect) notions as to the role of

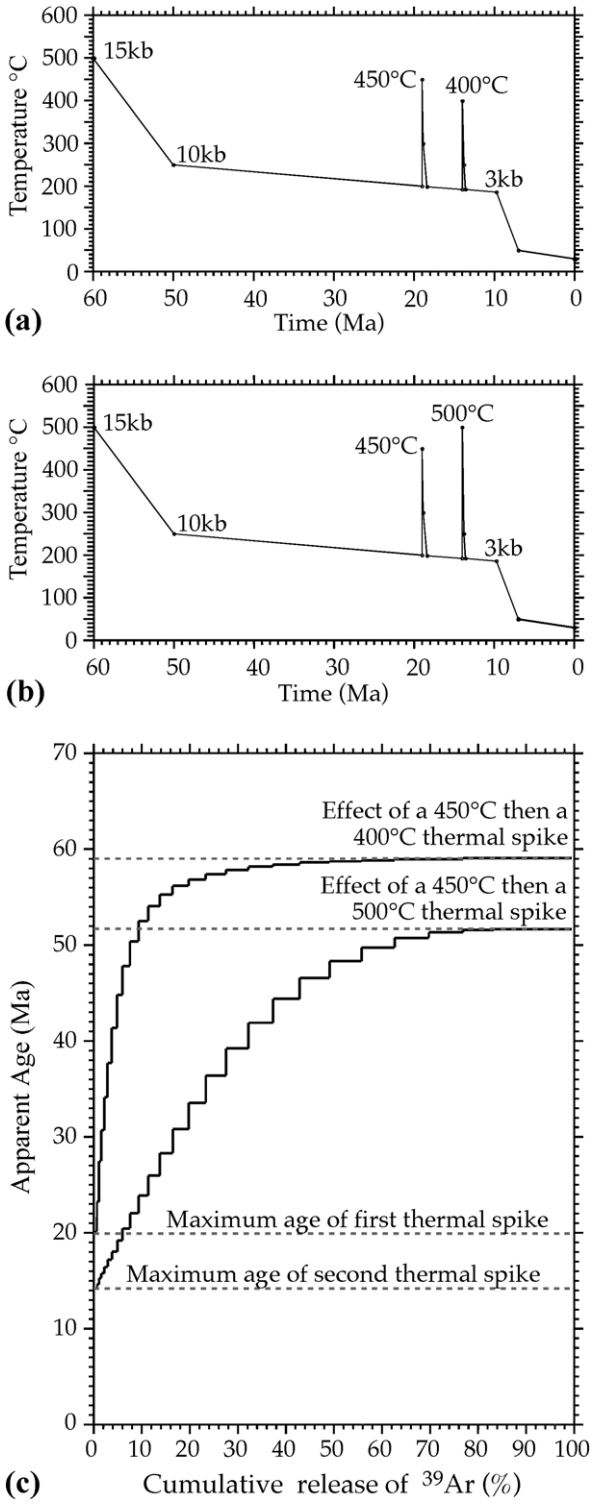

Fig. 1. A model phengite grown at 60 Ma is subjected to a sequence of thermal spikes ((a), (b)). Both thermal spikes involved temperatures well above the 'closure temperature' but complete degassing did not occur because the duration of the transient pulse in temperature was short. (c) Illustration of the pattern of gas release during the simulation of a step-heating experiment (using the MacSpectrometer in the *MacArgon* program; Lister and Baldwin, 1996). These simulations assume solid-state diffusion is the only mechanism by which degassing has taken place.

'closure temperature' (cf. Villa, 1998; Di Vincenzo et al., 2001).

These simulations do not take notice of important effects expected in real rocks (e.g. deformation and/or recrystallisation) or real effects in the mass spectrometer (e.g. dehydroxylation). Moreover they assume that solid-state diffusion is the only mechanism by which degassing has taken place. Such apparent age spectra are only to be expected if partial loss of argon occurs from a single class of diffusion domains (Turner et al., 1966; Wijbrans et al., 1995; Lister and Baldwin, 1996).

Nevertheless these idealized apparent age spectra define a sequence of ages that asymptotically converges towards an upward-bounding limit. This limit is here referred to as an 'asymptote', but it might also be approximated as a 'plateau' age if the limit was defined by a sufficient number of steps in the apparent age spectrum. It is clear that the 'plateau ages' inferred in the apparent age spectra that result from such experiments are no more than lower bounds for the original age of the material. This type of temperature–time history incidentally simulates variation that has been inferred for the Aegean metamorphic core complexes (Baldwin and Lister, 1998). Any such temperature–time history could have been used, however, for the purposes of this example.

It is evident that useful age information can be extracted by examining sequences of apparent ages in such experiments. The lower bound of ages recorded by the apparent age spectra is also useful, since it defines a downward-bounding limit that acts as maximum age. In the example illustrated this limit can be used to estimate the timing of the individual thermal pulses used to generate the individual apparent age spectra. The case of a downward bounding asymptote was first presented in Wijbrans and McDougall (1988, their fig. 10).

3. Asymptotes and limits in real data

We have begun by considering the pattern of gas release to be expected if: (a) solid-state (volume) diffusion is the mechanism that releases argon during a step-heating experiment in vacuo; and (b) volume diffusion was also the mechanism that released argon in nature during deformation and metamorphism, when argon escaped from the crystalline interior of mineral grains into the grain boundary network. These assumptions are not fundamental assumptions of the methods developed in this paper, however. It is not necessary for the diffusion behaviour during the step-heating experiment to replicate the behaviour of the mineral during deformation and metamorphism in the Earth. Mathematically speaking, all that is necessary is that volume diffusion be the dominant mechanism releasing argon, in both circumstances, and that the geometry of the diffusion domains remains constant. Alternatively, progressive dehydroxylation or defect diffusion during laboratory heating may take place in a manner that reveals gradients in argon concentration prior to any homogenisation caused by the destruction of the material (reviewer, pers. comm.).

In the example just illustrated (Fig. 1), volumetric (solid state) diffusion was the only mechanism allowing gas release, both in 'nature' and subsequently during the step-heating experiment. It might be argued that such simulations are of limited value, because white mica is known to dehydroxylate during step-heating experiments (e.g. Sletten and Onstott, 1998). Yet examples of similar apparent age spectra can be provided, nevertheless, obtained from real rocks, and using a real mass spectrometer, illustrating the same asymptotic convergence towards a limit.

3.1. Grenvillian shear zones in New Mexico

Heizler et al. (1997) have demonstrated the existence of asymptotically converging sequences in typical 'stair-case' spectra, comparing apparent age spectra from 1.4 Ga muscovite single crystals that have been variably affected by deformation in Grenvillian (~1.1 Ga) ductile shear zones (Fig. 2).

Fig. 2a shows a typical apparent age spectrum from a single crystal that was not deformed during later tectonism. A plateau age can be defined, allowing a reasonable approximation to the age of mineral growth, and/or subsequent rapid cooling. In comparison, partial loss of radiogenic argon during a later event becomes evident in apparent age spectra obtained from moderately deformed single crystals. In Fig. 2b deformation has led to partial argon loss but the original age of the mica grain is still evident. In contrast, strongly deformed single crystals yield apparent age spectra that display the effects of considerable partial loss (Fig. 2c and d). Heizler et al. (1997) demonstrated that the variation in apparent age could not be the result of recrystallisation.

These spectra strongly resemble those illustrated in Fig. 1, except in that the phenomenon of asymptotic approach to a limit is not as clearly evident. This might be expected, given the limitations of the measurement process, and the fact that dehydroxylation of the mica must have been taking place with increasing rapidity during the step-heating experiment (Sletten and Onstott, 1998). Nevertheless the form of the apparent age spectra can be accurately predicted by: (a) assuming that solid-state volumetric diffusion provided the (dominant) mechanism allowing release of radiogenic argon in nature; (b) considering the effects of partial argon loss only for a single class of diffusion domains; (c) assuming that volumetric diffusion was responsible for degassing during the step-heating experiment in the laboratory. It is difficult not to draw a comparison with simulated apparent age spectra as illustrated in Fig. 1, using *MacArgon* (version 6) (Lister and Baldwin, 1996) to predict the effect of partial loss of argon during a later short-lived thermal event.

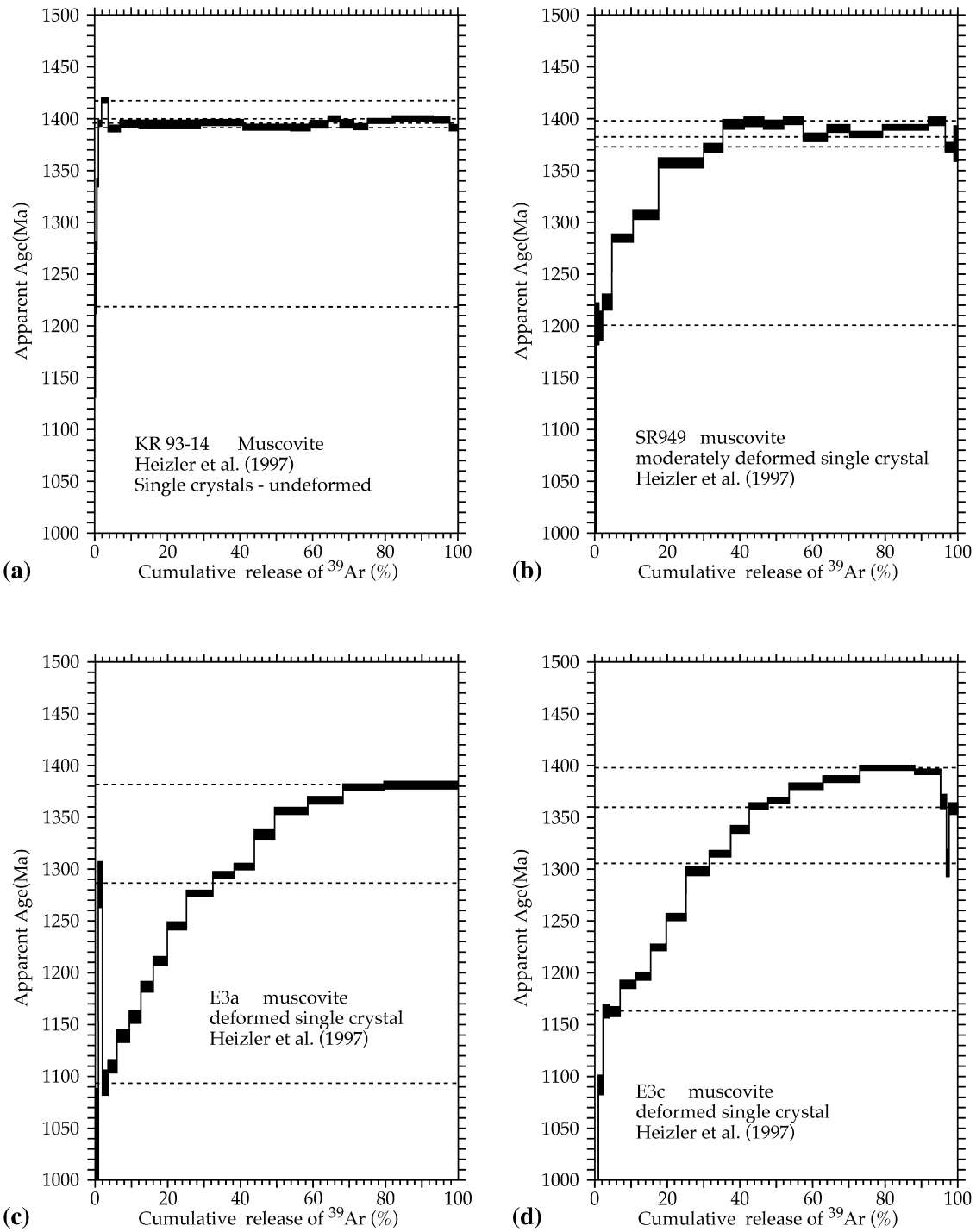

Fig. 2. Apparent age spectra measured by Heizler et al. (1997) from New Mexico: (a) relatively undisturbed spectrum from a single-crystal muscovite; (b) minor deformation leads to minor argon loss but the original age of the mica grain is still apparent; (c) and (d) show a higher degree of argon loss, from more deformed muscovite single-crystals. Asymptotes and limits allow estimates of the times that various events have taken place.

The apparent age spectra obtained by Heizler et al. (1997) from undeformed muscovite (e.g. Fig. 2a) can be interpreted to imply cooling below ~350–400 °C by about ~1.4 Ga, and continued cooling until ambient temperatures were below ~250–280 °C (cf. Baldwin and Lister, 1998). The age spectra from undeformed single crystals are relatively flat, and they show no effect that can be related to partial loss of argon during slow cooling, or during later thermal events.

Heizler et al. (1997) explain the disturbance seen in apparent age spectra measured from deformed mica in ductile shear zones by suggesting New Mexico experienced tectonism during the later Grenville Orogeny (at ~1.1 Ga). The ductile shear zones record microstructures that

developed during low greenschist facies conditions, requiring temperatures to have locally risen to 300–400 °C. The pulse in temperature that is thus inferred may have been sufficient to cause partial loss of radiogenic argon from deformed mica single crystals, in particular if their diffusion dimensions had been reduced as the result of deformation. The duration of the inferred Grenvillian thermal excursion must have been brief, otherwise partial loss would have been noticed in adjacent undeformed mica single crystals (including those with relatively small grain size). This short-lived thermal pulse may have had its origin in the effects of local shear heating in the Grenvillian ductile shear zones.

3.2. Mixing spectra from two microstructural reservoirs, Naxos, Greece

Another example of asymptotically converging sequences in real data is provided by apparent age spectra measured by Wijbrans and McDougall (1986, 1988) from the metamorphic core complex of Naxos, Cyclades, Greece (Fig. 3). These apparent age spectra reflect the effect of a short-lived thermal pulse on mineral grains relict from an older crystallisation event (Wijbrans and McDougall, 1986). Fig. 3a and b shows spectra that exhibit sequences of age steps that 'asymptotically' rise to a limit, and then decrease. In their pioneering studies, Wijbrans and McDougall (1986, 1988) proved effects related to distinct microstructural (and microchemical) reservoirs, demonstrating the influence of mixing between these reservoirs. This work strongly influenced the present study.

The shape of the apparent age spectra observed above cannot be simulated using simple volumetric diffusion based models. Wijbrans and McDougall (1986, 1988) demonstrate effects during the step-heating experiment related to the different behaviour of phengitic white mica as opposed to muscovite. The asymptotes and limits that can be defined in such spectra may have no geological significance because of the effects of 'mixing' of gas released progressively (but differently) from these distinct microstructural reservoirs (see Wijbrans and McDougall, 1986, their fig. 6). The ages that can be estimated are in fact lower bounds for the original age of the material, and statistical methods must be used to determine whether the ages obtained could possibly have any geological significance. Fig. 3c and d shows other spectra measured by Wijbrans and McDougall (1988) illustrating other patterns of gas release that consistently recur in apparent age spectra obtained from phengitic white mica, and which also may be the result of progressive release (and mixing) of gas from microstructurally (and/or microchemically) distinct reservoirs.

3.3. Mixing spectra from deformed K-feldspar, Ios, Greece

A final example to illustrate the nature of the asymptotically converging sequences that can be recognized in actual data is provided by apparent age spectra measured by Baldwin and Lister (1998) from the metamorphic core complex of Ios, Cyclades, Greece. Fig. 4 shows an apparent age spectrum from a Hercynian K-feldspar, first reset during Alpine high-pressure metamorphism, and then partially reset during later middle greenschist facies metamorphism associated with core complex formation. Different asymptotes and limits can be recognized in this spectrum, and these correspond to FMAs (frequently measured ages) determined from other apparent age spectra, regionally, and in the same dataset. Note that such saddle-shaped spectra may be the result of excess argon (McDougall and Harrison, 1999), but if excess argon is present, the age of the more retentive domain would not be expected to coincide with FMAs recorded throughout the dataset.

These apparent age spectra are frequently obtained from step-heating experiments with K-feldspar. McDougall and Harrison (1999) suggest that the initial steps of such a 'saddle-shaped spectrum' may be due to effects related to 'excess argon' and/or the lack of a correction factor to take in the effect of chlorine in the measurement process. The trough is due to the presence of a diffusion domain that is not as retentive as the remainder of the material. The older ages that are finally obtained are due either to the presence of a retentive domain (Baldwin and Lister, 1998) or to the presence of excess argon (McDougall and Harrison, 1999). Note that a gradual rise in apparent age occurs from the lower limit.

4. Apparent age spectra produced by mixing

Variation in the apparent age spectra described so far is a combination of two effects. On the one hand it is likely that subsequent deformation and/or thermal events have led to partial argon loss from existing diffusion domains, modifying age gradients in existing microstructural and/or microchemical domains. On the other hand it is evident that deformation and metamorphism have produced new microstructures (± microchemical variation) and thus a separate and distinct class of argon gas reservoirs that can be tapped separately during a step-heating experiment. A step-heating experiment thus releases gas from multiple reservoirs, and this may be described as mixing.

Several different mixing models can be conceptualised. We consider a sample in which there are two generations of white mica that have grown during different metamorphic and/or deformational episodes (e.g. a shear zone fabric in a micaceous schist, later refolded). Fig. 5 shows several different conceptual models for apparent age profiles that could be obtained by mixing gas released from two different microstructural reservoirs, as above, as the result of a combination of dehydroxylation and volumetric diffusion.

During a step-heating experiment gas may be released from both reservoirs, either progressively or episodically. One reservoir may release gas before the other, and dominate the early stages of gas release, while the other

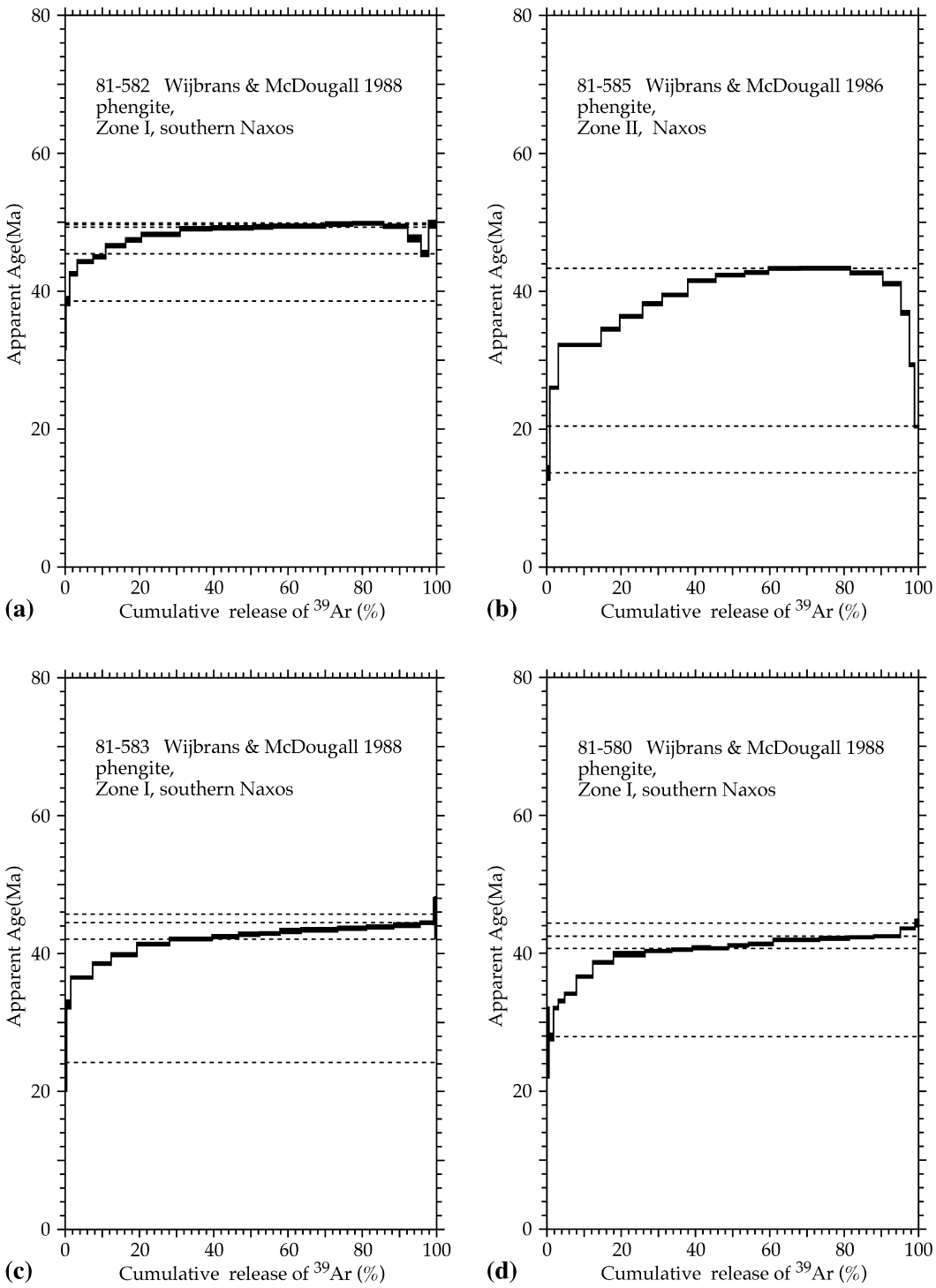

Fig. 3. Apparent age spectra measured by Wijbrans and McDougall (1986, 1988) from Naxos. Asymptotes and limits defined in this study are superimposed on each spectrum.

reservoir dominates later stages. The ideal case in which a retentive reservoir releases its gas after a much less retentive reservoir has degassed is first shown (Fig. 5a). This may be contrasted with progressive release from both reservoirs, initially as the result of a transition as the step-heating experiment reaches intermediate temperatures (Fig. 5b). Geochronologically useful information is still available. In Fig. 5a, one domain releases its gas and then the other, with little mixing. In Fig. 5b release from one domain occurs, then progressive mixing until release from the other domain dominates.

A complication is provided if there is early release of gas from the most retentive reservoir in nature prior to degassing of less retentive domains (Fig. 5c). Such a

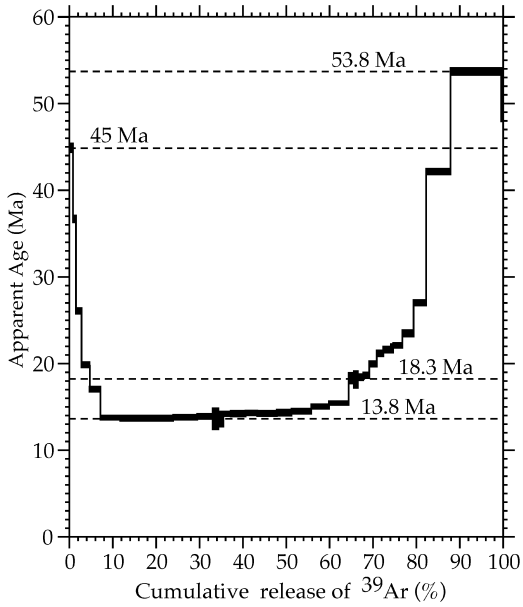

Fig. 4. Apparent age spectrum from a Hercynian K-feldspar (Baldwin and Lister, 1998) first reset during Alpine high-pressure metamorphism, and then partially reset during later middle greenschist facies metamorphism associated with core complex formation. Asymptotes and limits recognized in this spectrum correspond to FMAs (frequently measured ages) determined from other apparent age spectra, regionally, and in the same dataset.

retentivity reversal might be the result if one reservoir releases gas as the result of solid-state diffusion, while the other reservoir is tapped as the result of breakdown of the mineral structure during dehydroxylation. Only in the case of complete mixing is a result obtained that precludes useful information being derived from the step-heating experiment. In Fig. 5c the more retentive domain releases first and then the other domain, with little mixing. In Fig. 5d there is progressive mixing, while in Fig. 5e one reservoir immediately mixes with the other. In Fig. 5f there is sporadic and irregular sampling from one reservoir and then the other. Fig. 5g shows a plateau with an intermediate release dominated by the other reservoir. In Fig. 5h there is a retentivity reversal with a 'saddle'. In Fig. 5i an age profile is preserved in one reservoir, then the effects of a retentivity reversal become evident. Ambiguity is introduced if gas is released as the result of a smooth transition, with release of gas from one reservoir progressively diminishing while release from the other progressively increases (Fig. 5d).

It need not be assumed that gas released in the step-heating experiment is the result of solid-state diffusion. Dehydroxylation may result in complete mixing (Fig. 5e), or even intermittent and episodic sampling from one reservoir after the other (Fig. 5f). A retentive reservoir may be degassed abruptly (Fig. 5g) leading to deviation from an otherwise simple apparent age spectrum. Other complexities can be conceived, such as would result if the least retentive reservoir releases gas midway through degassing of the most retentive domain (Fig. 5h) or if the degassing of the most retentive domain reveals an apparent age gradient (Fig. 5i), interrupted by degassing of the least retentive domain, and then a retentivity reversal during which final degassing occurs.

Apparent spectra, as shown schematically in Fig. 5, could be analysed by the arbitrary definition of different plateau ages, but this would serve little purpose if an individual plateau was not well-defined. Of interest in this respect were complex apparent age spectra obtained by step-heating experiments in the Otago Schist (Forster and Lister, 2003). There are no well-defined 'plateau ages' in many of the age spectra illustrated, and there is considerable scatter between individual measurements in the step-heating sequence (Fig. 6). Such data might well have been discarded, except that several samples had been measured, and many individual steps across the total aggregate of samples had similar ages. What was interesting to us is that these FMAs could be predicted by defining asymptotes and limits to individual sequences and trends in the apparent age spectra. This paper is the result of further investigation of this aspect, with the realisation that it was possible to thereby provide the basis of a new method for the systematic interpretation of complex ^{40}Ar/^{39}Ar apparent age spectra obtained from separates of minerals in metamorphic tectonites.

Mixing spectra as illustrated in Fig. 5 may be characterized by approaches towards limiting ages (in this case defined by the age of gas in an individual microstructural reservoir). In the case of Fig. 5a the limits are well defined, and conventional analysis would have resulted in the recognition of one or more plateau ages. In the case of Fig. 5d no plateau would have been recognized but asymptotes and/or limits defined for the spectra would have approximated the age of the individual gas reservoirs. However, limits defined for the individual peaks and troughs in Fig. 5f would have been less successful with respect to providing estimates of the ages of the individual gas reservoirs. This is logical because, if mixing is random, one might not expect FMAs to be recognized.

A good example of the type of difficulty that might be expected comes from Wijbrans and McDougall (1986, their fig. 3, curve b). The asymptote or limit that can be defined at ~28 Ma is an artefact caused by competition of gas release from the two end member reservoirs (reviewer, pers. comm.). In this case, if several experiments had been performed, it might be predicted that variation in the age of the asymptote or limit would be obtained, even to the extent that a FMA would not have been defined. Conversely, if FMAs were obtained, these would need to be independently assessed to determine their significance.

It is important to note that asymptotes bound continuously rising or decreasing sequences of ages, and that they may represent a lower or, respectively, higher bound for the 'true age', which itself may not be represented in the age spectrum. In this case some variation in the ages obtained from different samples might be expected, for there would be no consistency in the ages recorded by different

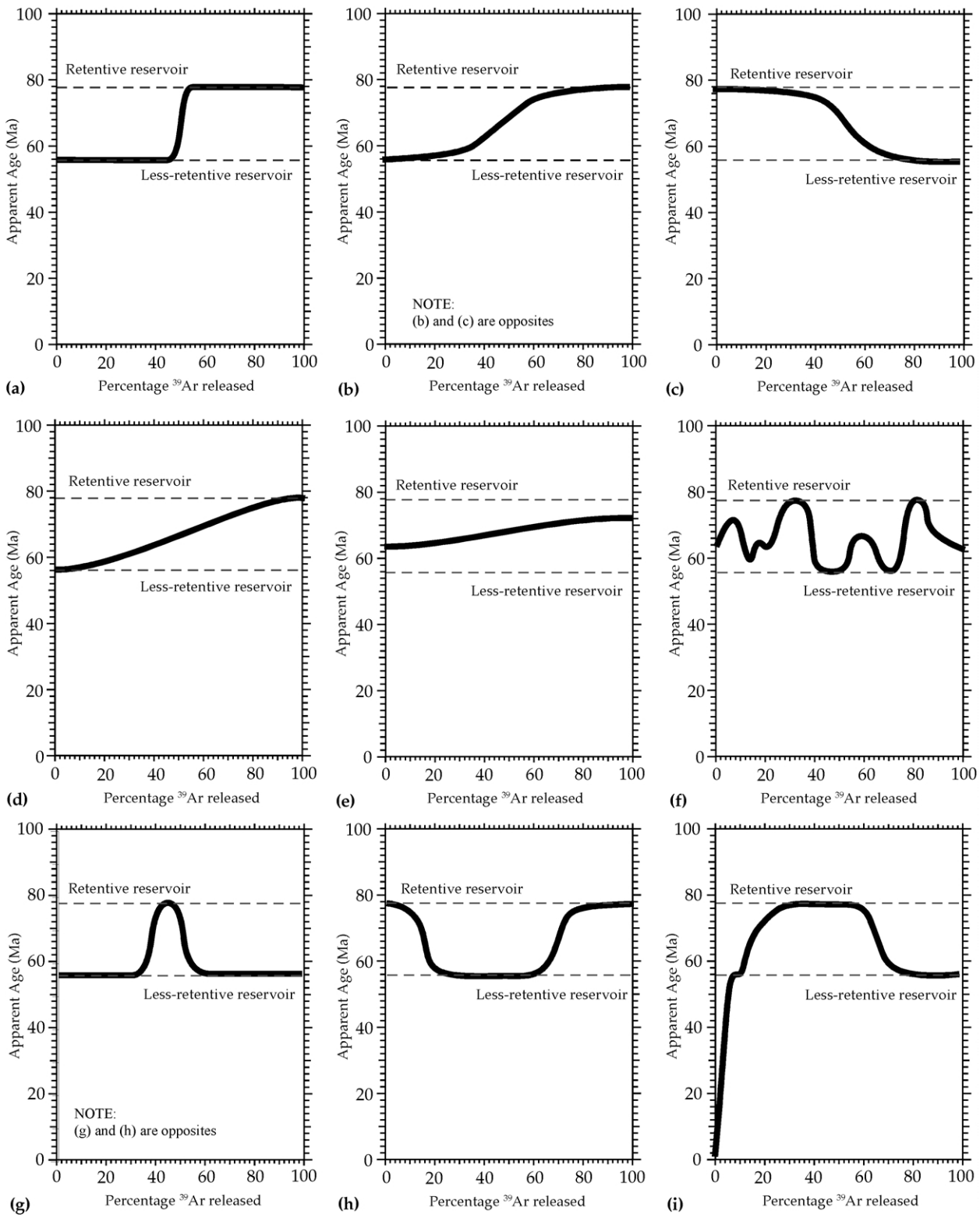

Fig. 5. Conceptual models for apparent age profiles obtained by mixing gas from two different microstructural reservoirs: (a) one domain releases and then the other, with little mixing; (b) release of one domain then progressive mixing until release from the other domain dominates; (c) the more retentive domain releases first and then the other domain, with little mixing; (d) progressive mixing; (e) one reservoir immediately mixes with the other; (f) sporadic and irregular sampling of one reservoir and then the other; (g) a plateau with an intermediate release dominated by the other reservoir; (h) a retentivity reversal with a 'saddle'; (i) an age profile preserved in one reservoir, then a retentivity reversal.

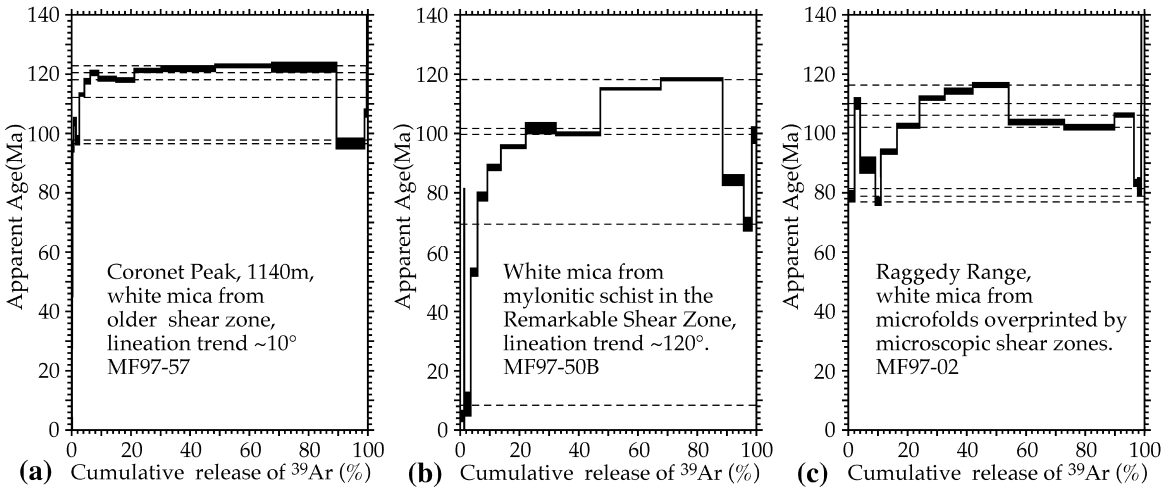

Fig. 6. Apparent age spectra from the central Otago Schist, New Zealand: (a) a shear zone from Coronet Peak, with a single recrystallization event (MF97-57); (b) a folded and partially recrystallised shear zone fabric from Mount Remarkable, with several generations of white micas in the microstructure (MF97-50B from the northern flank, at 1473 m); and (c) a folded and crenulated shear zone in the south of the Raggedy Range (MF97-02).

asymptotes or limits. An FMA is therefore unlikely to be obtained, but if consistency was obtained and an FMA resulted (providing at least a bounding constraint on the true age), again it would need to be independently assessed to determine its significance.

Under certain circumstances, however, individual FMAs will reflect the true age of different elements of the microstructure, or the timing of different events that affected the microstructure during the course of its history of deformation and metamorphism. Again, because of uncertainties described above, the significance of individual FMAs would need to be independently assessed, for example using in situ $^{40}Ar/^{39}Ar$ laserprobe experiments, or alternative geochronological methods.

5. The method of asymptotes and limits

To develop the method described in this paper we needed a systematic approach that would allow us to extract asymptotes and limits from a collection of measured apparent age spectra, to plot the results, and then to determine the significance of any FMAs that might have been obtained by application of the technique. The first step requires extraction of asymptotes and limits from a collection of measured apparent age spectra. To this end the following definitions have been adopted.

An *upward-bounding asymptote* is defined by a sequence of steps in the apparent age spectrum that progressively increase in their apparent age, but level out asymptotically against an upper limit. For practical purposes the asymptote is taken as the uppermost step in the sequence. From the theoretical standpoint it is evident that an (upwardly bounded) asymptotic limit is a minimum age, allowing an estimate of the original crystallisation age of the material.

A similar definition applies for a *downward-bounding asymptote*, but the sequence of age steps is considered in reverse. The steps in the apparent age spectrum fall and level out at a younger age. The asymptote is taken as the lowermost step in the sequence, and represents a maximum possible age, constraining the timing of individual events later in the history of the material in question. *Intermediate asymptotes* may be defined by a sequence of apparent age steps that first converge and then diverge. These are the most difficult to determine accurately in a step heating sequence.

Limits can also be recorded. Limits are defined that bound sequences of increasing (or decreasing) ages in the apparent age spectrum. *Downward-bounding limits* are defined by apparent age steps that first decrease and then increase. *Upward-bounding limits* are defined by apparent age steps that first increase and then decrease.

The significance of limits is thus open to debate. At least, if limits are systematically recorded throughout a dataset, it is possible to assess whether or not the ages recorded have statistical significance.

We can provide examples of each of these asymptotic sequences. For example Fig. 1 illustrated upward-bounding asymptotes for a theoretical example, to demonstrate the effectiveness of the method in an ideal case. The first simulation involves the effect of thermal pulses that briefly reach 450 °C and then 400 °C. Temperature after each pulse decreases rapidly back towards ambient with a thermal decay constant of 0.1 Ma (Fig. 1a). This sequence causes relatively little degassing. An upward-bounding asymptote could be defined in the apparent age spectrum, and this estimates the age of the model phengite to be 59.1 Ma (Fig. 1c). This is the same age as would be recorded by an asymptote drawn for the same model phengite when subject to the same overall temperature–time history, but in this case without the effect of thermal spikes being considered (not shown in Fig. 1). The greatest argon loss occurs for the

simulation in which the second thermal pulse reaches 500 °C. Note that the upward-bounding asymptote that can be defined in this apparent age spectrum significantly underestimates the age of the model phengite (Fig. 1b and c).

The apparent age spectra measured by Heizler et al. (1997) provide excellent examples of upward-bounding asymptotes (or limits) in apparent age spectra measured from naturally occurring white mica (Fig. 2). The estimates of age provided by the asymptotes or limits again underestimate the crystallisation/cooling age as recorded by the undeformed single crystals (Fig. 2a).

Downward-bounding asymptotes are often recognised in apparent age spectra measured from K-feldspar (e.g. Fig. 4), where the release of gas from the least retentive domains often yields a saddle-shaped spectrum. The initial steps may release gas that was adsorbed from the pore fluid and released from low retentivity pathways, or result from excess argon released from fluid inclusions (McDougall and Harrison, 1999). Gas released from the least retentive domains is responsible for the trough of the 'saddle'. Thereafter apparent age begins to increase as gas is released from the more retentive diffusion domains (Lovera et al., 1989; Harrison et al., 1993). Gas released in the final high-temperature steps can represent excess argon, producing a U-shaped apparent age spectrum. This may be due to the interference of excess argon, or from interference due to chlorine (McDougall and Harrison, 1999), which creates artificially high apparent ages. Fig. 4 shows such an apparent age spectrum, using as an example data from a Hercynian K-feldspar, from the Aegean metamorphic core complex of Ios, Cyclades, Greece (Baldwin and Lister, 1998). Note, however, that the ~50 Ma age for the most retentive domains can be confirmed using apparent age spectra measured from phengite in the same samples.

Downward-bounding asymptotes may also develop as the result of recoil processes in a sample with mixed high-K and low-K reservoirs (Koppers et al., 2000).

6. Frequently measured ages (FMAs)

To provide a concrete example of the further application of the method, and its use in determining FMAs, complex apparent age spectra measured from the Otago Schist (Fig. 6) were subjected to further analysis. First each asymptote or limit recognised in these apparent age spectra have been plotted, tabulated in an Excel table, and attributed a specific percentage of the total gas released during the step-heating experiment.

It is possible to weight each asymptote or limit equally in this tabulation, but this takes no account of the potential variation in the relative magnitude of individual gas reservoirs. To eliminate bias it is necessary to eliminate asymptotes or limits that are defined by relatively small gas percentages. One can estimate the relative volumes of different reservoirs in an ideal circumstance, but this becomes subjective in other cases. We opted therefore to weight each asymptote or limit by the percentage of gas released during the final step that defines the asymptote or limit. At least this allows a procedure to be defined that can be automated (for example in the successor to *MacArgon* (Lister and Baldwin, 1996), *JavArgon*, currently under development).

This decision means that we will consistently underestimate the relative volume of the most substantial gas reservoirs, but the advantage is that limits defined by $<1\%$ of the total gas release can be included at the same time as a plateau or asymptote defined by 10–20% of gas release without undue bias being introduced. There are some aspects of the method that are therefore not satisfactory, since statistical analysis of the significance of asymptotes and limits requires a relatively accurate estimate of the percentage of gas released that can be attributed to a particular gas reservoir.

The Excel table that results from this analysis lists the age (Ma) of the asymptotes and limits in one column with their attributed gas release percentage in another. The final step is to plot a frequency–magnitude plot for the asymptotes and limits defined for each age spectrum (Fig. 7). To do this each asymptote or limit is weighted by the attributed percentage of gas (see above), and smoothed according to a normal distribution, with an arbitrarily determined standard deviation (e.g. 0.5 Ma). Individual percentage-gas-weighted distributions are then summed, to define the frequency–magnitude plot for an individual apparent age spectrum. In the present study this summation was performed using a modified version of the *MacArgon* program (version 7). The program was designed to read Excel text/tab delimited tables.

Such an analysis needs to be repeated for each of the individual apparent age spectra in a dataset, and from this data statistically significant FMAs can be identified by summing the individual frequency–magnitude plots (Fig. 8). Such a method of analysis means that it is possible to reduce bias and/or interpretation, but more data rather than less will need to be recorded. If statistical analysis is performed with a sufficiently large dataset and well-defined FMAs are obtained, these are then more likely to reflect geologically meaningful events.

The phenomenon of FMAs defined by the statistical analysis of limits and asymptotes to age sequences in complex $^{40}Ar/^{39}Ar$ apparent age spectra is not uncommon. Well-constrained FMAs have been discerned for example in apparent age spectra measured from the Lachlan Fold Belt, in Eastern Australia (Foster and Gray, 2000) or from Syros (Baldwin, 1996). These authors provide synoptic plots of the apparent age spectra that they have measured, but these are very difficult to interpret because overlap leads to an inability to extract information from an individual age spectra, with added confusion caused by the error bars on each step obliterating other information.

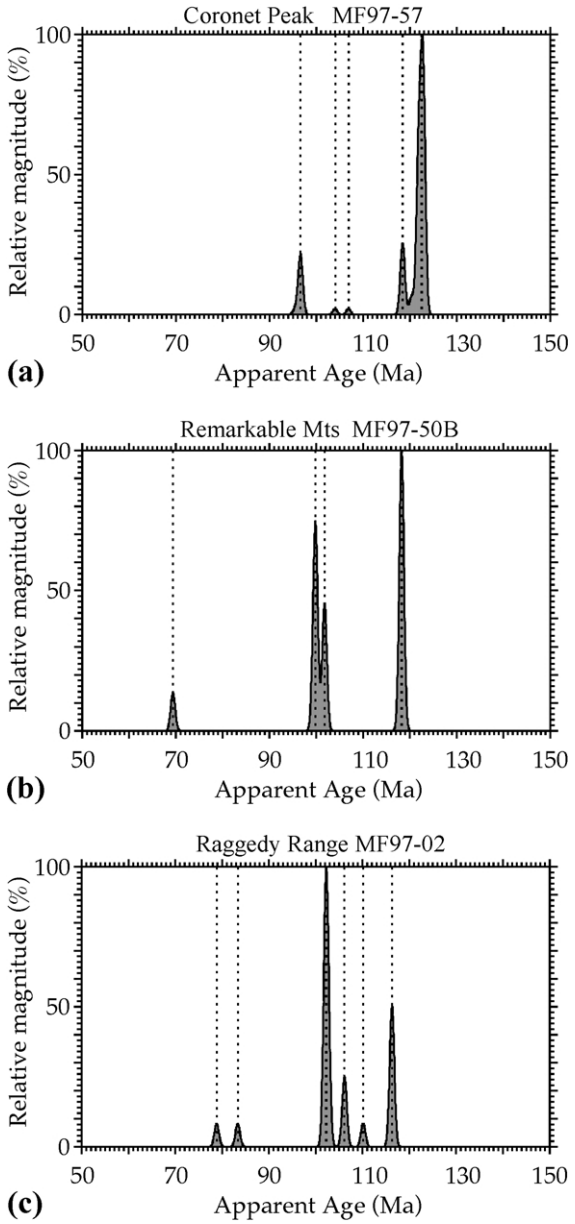

Fig. 7. Frequency–magnitude plots of gas-weighted asymptotes and limits recognised in $^{40}Ar/^{39}Ar$ apparent age spectra measured from shear zones and folded shear zones in the central Otago Schist, New Zealand. Data from: (a) a shear zone on Coronet Peak (MF97-57); (b) a folded and crenulated shear zone fabric on Mount Remarkable (MF97-50B); and (c) a folded and crenulated shear zone in the south of the Raggedy Range (MF97-02).

Foster and Gray (2000) and Baldwin (1996) interpret their data to imply continuous process over the time interval in question. Nevertheless examination of the published plots using techniques as described in this paper reveals that many individual steps in the apparent age spectra coincide, and there are distinct clusters in the apparent age population. Application of the method of asymptotes and limits to these datasets has revealed distinct clusters in the age data that may well reflect distinct geological events.

7. Apparent age and microstructure

The samples illustrated from the Otago Schist were microstructurally complex. In spite of this complexity a consistent correlation could be inferred between apparent age variation and individual microstructural reservoirs. For example Fig. 6a is an apparent age spectrum obtained from a sample of the oldest shear zone fabric recognised in the central Otago Schist on Coronet Peak (see Forster and Lister, 2003). This oldest generation of shear zone fabric is extensively recrystallised (Fig. 9a), with garnet + biotite + white mica assemblages locally developed. This implies that these shear zones reached middle greenschist facies ($>\sim$450 °C).

In a sample from the adjacent Remarkable Mountains, the same, or a similar shear zone fabric is folded and decussately recrystallised (Fig. 9b). This sample yields a more complex apparent age spectrum (Fig. 6b), perhaps reflecting progressive mixing of argon released from two distinct microstructural reservoirs. Nevertheless the contribution from the older shear zone fabric can still be recognised.

A third sample taken from a structural location similar to that of the sample from the Remarkable Mountains developed a similar sequence of fabrics and microstructures. The older shear zone fabric is tightly crenulated and decussately recrystallised. At least two microstructural reservoirs can be thus inferred. The apparent age spectrum (Fig. 6c) displays similar ages as can be recognised in the sample from the Remarkable Mountains, but now the order in which the two microstructural reservoirs have degassed can be interpreted to have reversed. This produces a pattern of age variation that is not unlike that illustrated in Fig. 5i. The variation observed can be ascribed to the effects of a retentivity reversal during the step-heating experiment.

As part of a detailed study Forster (2002) showed that individual FMAs determined in this dataset (Fig. 8) could be correlated with specific microstructural reservoirs. Several distinct generations of shear zone fabrics were recognised and it has been demonstrated that each of these each yield characteristic ages. FMAs that can be recognised in step heating experiments performed on more complex microstructures consistently correlate with distinct shear zone fabrics in individual samples. These correlations need to be confirmed by independent geochronological measurements using another isotope system (e.g. Rb/Sr), or an in situ analysis using a laserprobe to determine whether particular FMAs can be correlated with the age of an individual microstructural or microchemical reservoir. Preliminary results provide reassurance in respect of the ability of the method to extract significant ages from a complex dataset.

8. Discussion

8.1. Microstructural reservoirs

Radiogenic argon can be released sequentially from

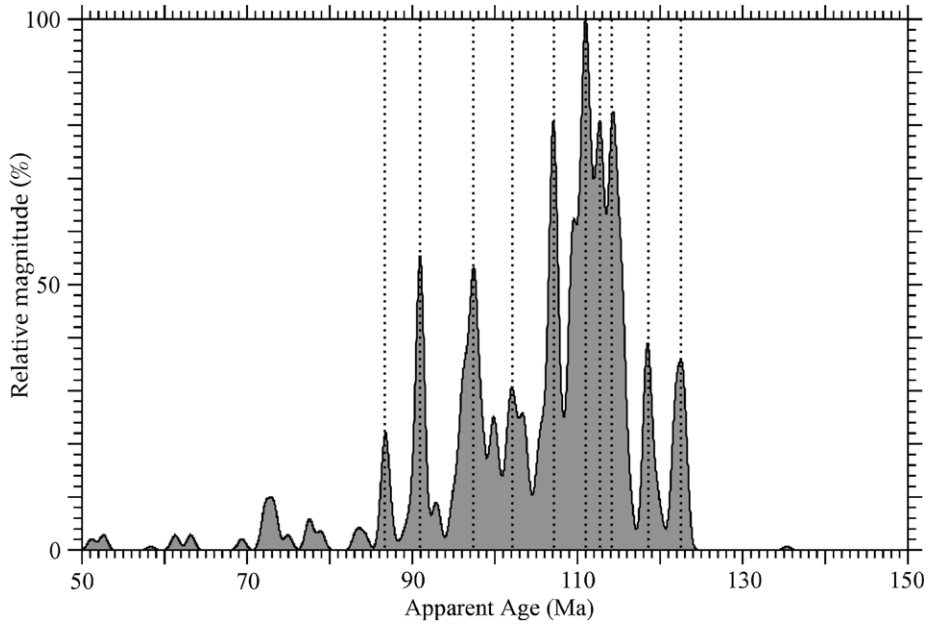

Fig. 8. A frequency–magnitude plot from the complete dataset of $^{40}Ar/^{39}Ar$ apparent age spectra from the Otago Schist samples measured by Forster (2002). The peaks marked with the dotted lines mark the FMAs determined from these samples.

different microstructural reservoirs as the result of several processes during the course of a step-heating experiment. These processes include solid-state diffusion, dehydroxylation, decrepitation of fluid inclusions, and/or simple degassing from low-retentivity adsorption sites. The pattern of gas release might depend on the progress of dehydroxylation reactions in collaboration or in competition with release as the result of volumetric (solid-state) diffusion. Many different circumstances might apply. In summary, however, if a step-heating experiment can be designed so that the argon release process systematically samples one reservoir, then another, the apparent age spectra that are produced will be capable of providing useful information with respect to the age of different microstructural reservoirs.

The development of distinct microstructural reservoirs during deformation and recrystallisation is not difficult to envisage, for example as illustrated schematically in Fig. 10 for single crystals of white mica, illustrating different styles of deformation and recrystallisation as they affect white mica. Microchemical changes commonly take place during such recrystallisation (e.g. Hames and Cheney, 1997). Note that recrystallisation in the sense it is used here refers in the main to the effects of grain boundary migration (Urai et al., 1989). Rotation recrystallisation is unlikely to have any effect except indirectly with respect to allowing modification of diffusion dimensions, as for example may have been the case with respect to the mica in the Grenvillian shear zones discussed by Heizler et al. (1997).

White mica can be either folded (Fig. 10a) or torn and sheared (Fig. 10c) before it is recrystallised. Fig. 10a illustrates a white mica grown during an earlier metamorphism but then caught in the shortening field of a later deformation. Folded mica cleavage books are affected by grain boundary migration in limited areas (shown shaded). A later metamorphism may lead to a second period of recrystallisation, involving grain boundary migration, and new white mica growth. A surface free energy dominated decussate texture is produced (Fig. 10b). Mica in the shaded area might yield an age that reflects the second period of mineral growth, because it has been regrown. However, relicts of the original mica (shown in Fig. 10a) are still present (in the regions shown unshaded). These relicts may yield older ages if temperatures remained low enough to allow radiogenic argon to be retained.

Similar effects are to be expected in white mica that has been caught in the extension field of a later flow, where mica 'fish' result (Lister and Snoke, 1984). The boundary region is sheared, and partial loss of radiogenic argon will occur because diffusion dimensions have been reduced, decreasing the retentivity of the material (Fig. 10c). Grain boundary migration and subsequent grain growth leads to microstructures as shown (Fig. 10d). This recrystallisation may occur with or without microchemical changes behind the migrating grain boundary (Scaillet et al., 1992). Radiogenic argon trapped in the lattice of the original material will be lost to the grain boundary network as it is passed over by the migrating boundary. In consequence, the new grown mica (shaded) will yield an apparent age that reflects the younger period of mineral growth. Again the cores of the 'mica fish' may yield older ages if temperatures remained low enough to allow radiogenic argon to be retained. The new grown mica will reflect the age of the shear zone.

Grain boundary migration is an efficient mechanism

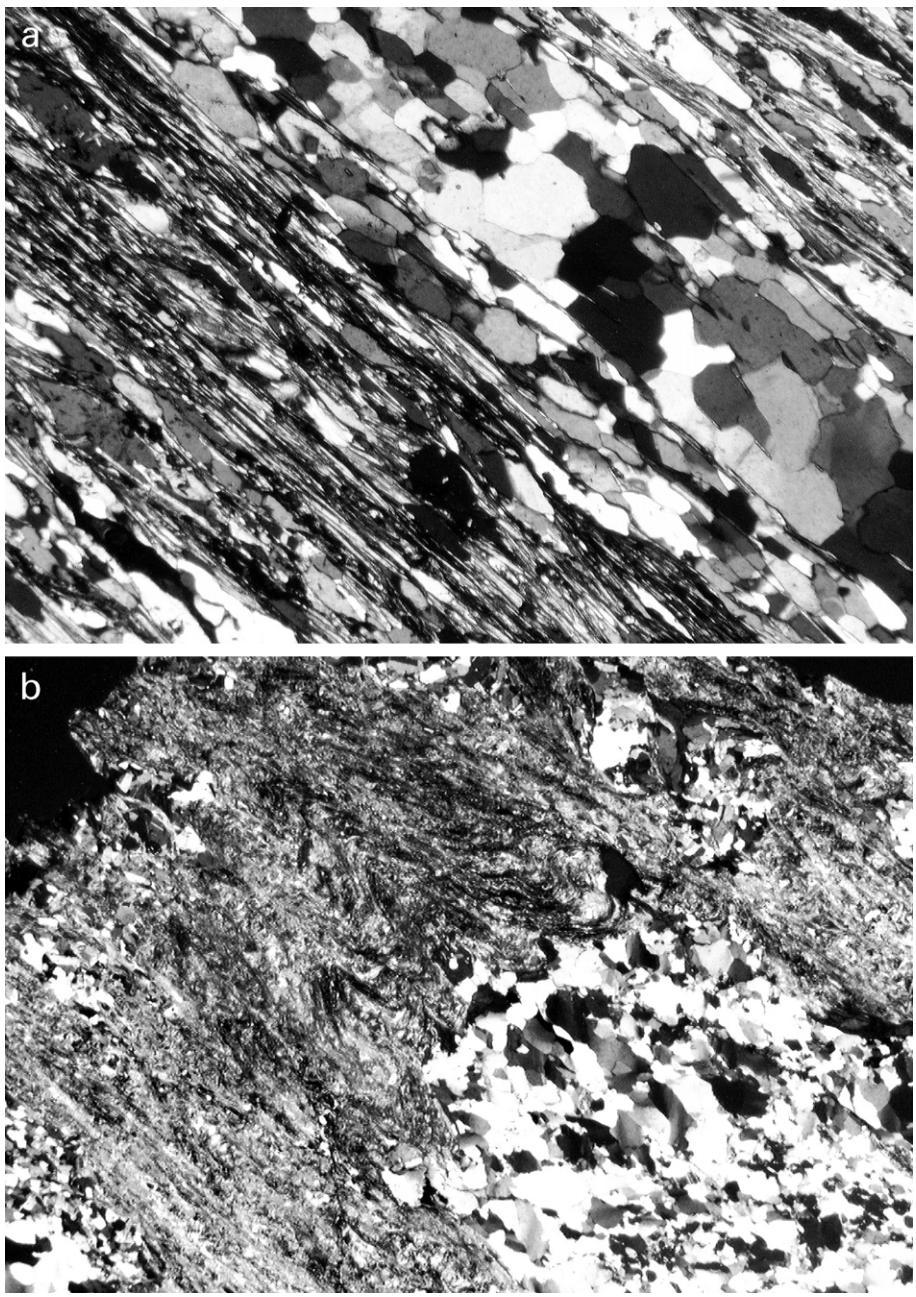

Fig. 9. (a) Microfabrics developed in an intense shear zone at Coronet Peak, Otago Schist, New Zealand. Quartz lenses display foam textures (photo taken in crossed polarized light). Sample MF97-57. Field of view ~2 mm. (b) A micro-scale hinge zone with an overprinting crenulation cleavage (photo taken in crossed polarized light), from Mount Remarkable, Otago Schist, New Zealand. The older shear zone fabric has been tightly crenulated and decussately recrystallised. New mica grains have grown with (0001) parallel to the axial plane of these crenulations. Sample MF97-50B. Field of view ~12 mm.

allowing micro-chemical change during metamorphism. Such changes behind a migrating grain boundary may reflect decreasing pressure during the recrystallisation history of a phengite, for example. These microchemical changes may be significant in that the newly grown material may have different intrinsic diffusion parameters (e.g. frequency factor, D_o, activation energy, E, or activation volume, $\bar{v}$) in comparison with the material that was replaced. The newly grown material may therefore define a distinct microstructural reservoir with different retentivity, and/or distinctly different susceptibility to dehydroxylation during later step-heating experiments in the mass spectrometer.

Similarly the effects of deformation introduce a substructure (dislocation tesselations and/or subgrain networks) that may affect the effective diffusion dimensions, decreasing the retentivity of the material and/or fundamentally changing the susceptibility of the material to dehydroxylation reactions (see Fig. 11). Different parts of the microstructure may therefore preferentially release

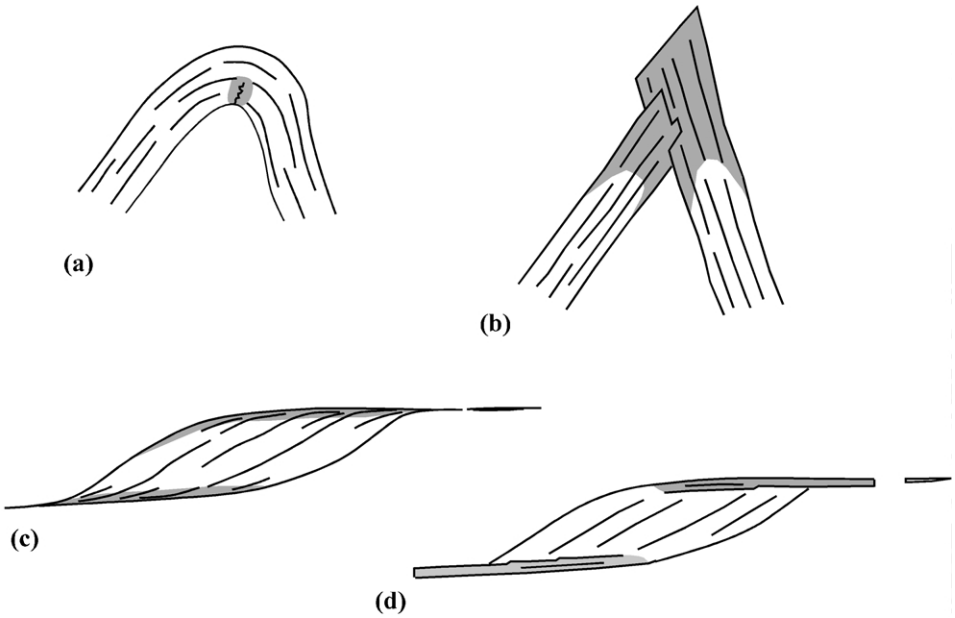

Fig. 10. Different styles of deformation and recrystallisation as they affect white mica. (a) Crenulation in the shortening field of a later deformation, with grain boundary migration in limited areas (shown shaded). In (b), a later metamorphism leads to a second period of recrystallisation and white mica growth, producing a decussate texture. In (c), a mica 'fish' is caught in the extension field of a later flow. In (d), recrystallisation leads to grain boundary migration and new grain growth. The new grown mica (shaded) will yield an apparent age that reflects the younger period of mineral growth. Relicts of the original mica will yield older ages.

radiogenic argon, and thus produce complex apparent age spectra as the result of mixing.

8.2. The Argon Partial Retention Zone

Many of the effects discussed in this paper suggest that the white mica involved has deformed and/or recrystallised in an Argon Partial Retention Zone (PRZ) Solid-state diffusion within a potassium-bearing mineral grain in an Argon PRZ takes place at a rate that is fast enough to ensure significant diffusional loss of ^{40}Ar to the grain boundary network, particularly from the rims of individual diffusion domains, but not so fast as to prevent a mineral from retaining most of its radiogenically produced ^{40}Ar. Temperatures are high enough to allow partial gas loss, but not so high as to reset the argon 'clock' during the interval of time in question. At the same time conditions in an Argon PRZ are essentially those required to encourage the onset of pervasive ductile deformation, fabric development, metamorphic mineral growth and recrystallisation. The reason for this coincidence may be an underlying dependence on the rate of intracrystalline diffusion of certain atomic

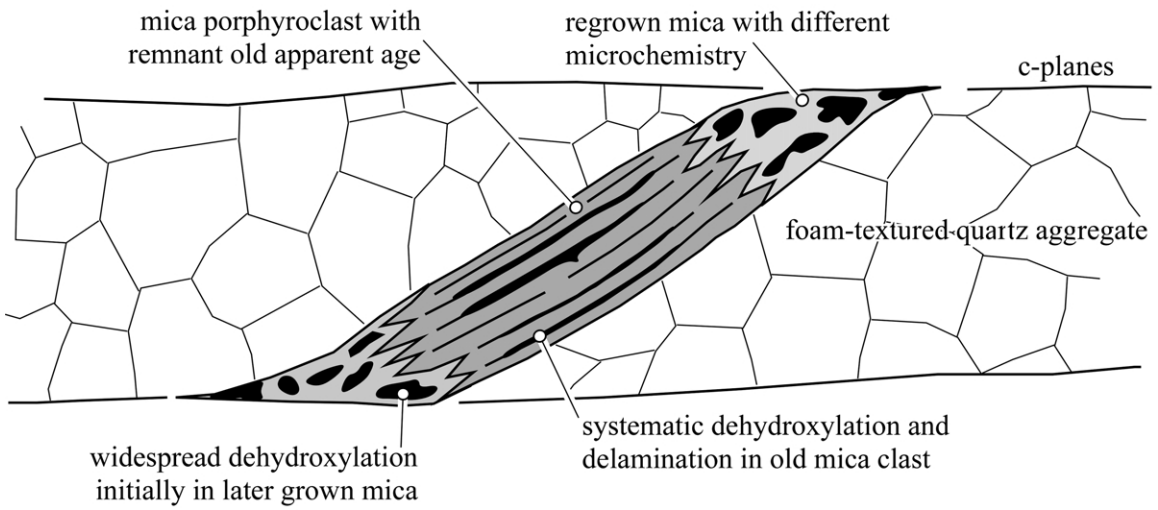

Fig. 11. Dehydroxylation reactions progressively destroy a microstructure with two components, initially releasing gas dominantly from domain B. In the later stages, delamination and dehydroxylation have 'decorated' diffusion domains in the older porphyroclast, and reaction fronts sweep progressively from rim to core.

species (e.g. oxygen). But whatever its cause, this coincidence offers a significant opportunity in terms of geochronology, enabling potential correlation between a measured apparent age spectrum and microstructure.

The concept of the Argon Partial Retention Zone stems from Baldwin and Lister (1998) who introduced "the concept of the argon partial retention and resetting zone (PRZ)". These authors restricted the definition of the Argon PRZ to "stable continental crust characterized by a constant geothermal gradient" and defined the PRZ as "that portion of the crust where temperatures are insufficient to completely reset argon-systematics within pre-existing potassium bearing minerals". This definition allows precise constraint as to the extent of the Argon PRZ, but this will be different for each mineral considered.

8.3. Dehydroxylation and delamination during step heating

The central issue we confront in advocating a systematic approach to the analysis of apparent age spectra produced from white mica relates to uncertainty as to the effects of dehydroxylation and delamination during step-heating in vacuo. There is a general perception that these phenomena preclude the extraction of geologically useful information from a step-heating experiment, whereas in fact this need not be so. Sletten and Onstott, 1998) write that: "The rates of delamination in vacuo and the rate of Ar diffusion for muscovite in nature…both depend upon its chemical composition, structural integrity, and grain size". These authors demonstrate that dehydroxylation and delamination preferentially affect smaller grain sizes, and therefore that a step heating experiment may systematically reflect variation of apparent age in different microstructural and/or microchemical reservoirs.

This means that a carefully designed step-heating experiment for "a compositionally or structurally heterogeneous population of grains, such as muscovite from shear zones" will yield apparent age spectra that "may be able to detect intergranular variations" in apparent age (Sletten and Onstott, 1998). Distinct microstructural and/or microchemical domains (e.g. as described by Hames and Cheney (1997)) may be preferentially degassed during a step-heating experiment. Apparent age spectra may thus reflect variation that correlates with the microstructure. Note that some of this microstructural variation in apparent age will readily be revealed by modern laser spot fusion analyses (e.g. Hames and Cheney, 1997). However, this does not preclude the possibility that conventional step-heating experiments will also reveal the existence of distinct microstructural reservoirs, in particular if sufficiently detailed experiments are undertaken with several initial steps in the range 500–700 °C (e.g. as is the case for experiments reported by Heizler et al. (1997)).

8.4. Solid-state diffusion during dehydroxylation?

In considering the implications of systematic release of argon from white mica in a step-heating experiment, it also needs to be considered that, although dehydroxylation may well take place during a step-heating experiment, it is not uncommon that apparent age spectra are produced that are typical of volumetric (solid-state) diffusion. Wijbrans and McDougall (1986) note: "The shape of (an) age spectrum is very similar to that which would be predicted on the basis of diffusion theory if, subsequent to crystallisation, argon was lost by volume diffusion in a discrete event". Heizler et al. (1997) compared apparent age spectra from 1.4 Ga muscovite single crystals variably affected by deformation in Grenvillian (~1.1 Ga) ductile shear zones. Apparent age spectra from single crystals that were not deformed during later tectonism (Fig. 2a) can be compared with age spectra from single crystals that were moderately deformed (Fig. 2b), or strongly deformed (Fig. 2c and d). The deformed material yielded apparent age spectra typical of those that result in partial loss by solid state diffusion from a single diffusion domain. Apparent age spectra with a similar form to those produced by Heizler et al. (1997) can be produced using *MacArgon* to simulate the effect of gas release during a later (short-lived) thermal event (Lister and Baldwin, 1996).

There is no doubt that white mica decomposes (by delamination and dehydroxylation) during step heating experiments in a vacuum. Yet Heizler et al. (1997) were able to perform several experiments on the same or similar material, and obtain comparable if not identical results. Similarly Sletten and Onstott (1998) produce an apparent age spectrum from heated blocks of muscovite that is entirely consistent with predictions made on the basis of the assumption that volumetric diffusion has caused partial degassing of radiogenic argon (their fig. 3d). The apparent age spectrum is as expected for a single diffusion domain degassing during the step-heating experiment, with solid-state diffusion providing the mechanism allowing release of radiogenic argon. In the Otago Schist, Forster (2002) recorded a broad similarity of apparent age spectra obtained from different locations, in particular from samples subjected to the same history of deformation and metamorphism at similar structural levels.

We conclude that a systematic process must be involved during step heating experiments, even though argon released into the mass spectrometer is likely to be derived from the effects of both solid-state diffusion and dehydroxylation. We therefore suggest that a carefully fashioned step-heating experiment may allow dehydroxylation to progressively 'decorate' a microstructure (in the same way that etchants released onto a polished surface may 'decorate' a microstructure). Different parts of the microstructure may dehydroxylate at different times (Fig. 11), so that the results of a step-heating experiment reflect

progressive mixing of gas released from different elements of the microstructure.

Sletten and Onstott (1998) showed that for step heating in vacuo, the effects of dehydroxylation will not be detected for steps below 700 °C (at least for coarse grain sizes). They conclude that "incremental heating analyses in this range may yield geologically useful information" (both with respect to fossil concentration gradients in radiogenic argon as well as with respect to the kinetics of the processes involved). At higher temperatures they note that "distortions in the muscovite lattice produced by the partial conversion to muscovite dehydroxylate are not as drastic as those produced by dehydrogenation and dehydroxylation of amphibole and biotite". Delamination takes place along cleavage planes by 750 °C, and is significantly more intense (based on the distances between cleavage planes) by 860 °C. By 1025 °C the sample was intensely delaminated with sheets as thin as 0.5 μm. Heating at 1100 °C eventually destroys the remaining vestiges of the muscovite structure, producing interlocking aggregates of mullite and corundum (see references in Sletten and Onstott (1998)). These experiments showed that the rate of argon release during the step-heating experiment was consistent with the observed rates of dehydroxylation and delamination, in particular for heating steps above 700 °C.

Sletten and Onstott (1998) also suggest that "Ar diffusion from thin dehydroxylated slabs may dominate the Ar release mechanism for temperatures above 900 °C". This pattern of gas release suggests that diffusion is involved in the low temperature steps as well as in the high temperature steps (although a different material is then involved). Dehydroxylation and delamination may thus systematically sample existing diffusion domains, particularly if their shapes are defined by thin sheets parallel to the cleavage. Individual sheet-like diffusion domains would most likely be bounded by incipient cleavage planes, and dehydroxylation fronts once formed might then be expected to systematically advance, progressively releasing gas from rim to core (Fig. 11). If sheet-like diffusion domains are involved, diffusion during the step-heating experiment, even at an accelerated rate as would occur in a modified dehydroxylate crystal structure, will mimic the argon release pattern necessary to reveal the existence of fossil gradients in the concentration of radiogenic argon.

8.5. The shape of diffusion domains in white mica

There are many aspects of argon geochronology in muscovite that are better explained by the assumption that the rate-determining step involves diffusion parallel to the *c*-axis in slab-shaped diffusion domains. Experiments performed by Robbins (1972) have been reanalysed by Lister and Baldwin (1996). Only a small subset of the data was internally consistent, however, and this subset was shown to require the assumption of slab-shaped diffusion domains. We perhaps need to reconsider the assumption that diffusion domains in muscovite are approximated by cylinders parallel to the *c*-axis.

Many of the difficulties highlighted by Sletten and Onstott (1998) would be resolved if diffusion of argon parallel to the *c*-axis was the rate limiting step, both for naturally occurring muscovite and for dehydroxylated sheets of mica formed during step-heating. Since the spacing of incipient cleavages will vary across large mica grains, it is possible to explain variation in apparent ages obtained in laser spot fusion analyses, in particular when this data does not vary in a way that would be predicted assuming cylindrical geometries (e.g. Hames and Bowring, 1994; Hodges et al., 1994; Hames and Cheney, 1997; Sletten and Onstott, 1998).

A model requiring slab-shaped diffusion domains in white mica implies migration of argon across the (distorted) octahedrally co-ordinated Fe/Mg layers. Sletten and Onstott (1998) recognize that release of argon may be accelerated by short-circuit diffusion parallel to (0001). An additional diffusion step may be required to allow ^{39}Ar to penetrate the octahedral layer although crystal chemical considerations might at first glance rule out this possibility (Dahl, 1996). Sletten and Onstott (1998) advance an explanation of 'stair-case' spectra based on the effects of recoil. The intricacies of this model serve only to illustrate the fundamental nature of the uncertainties involved.

Age gradients are commonly observed in apparent age spectra from white mica, and these 'stair-case' patterns resemble spectra that are the result of volumetric (solid-state) diffusion. Whatever process is responsible for the production of age gradients in apparent age spectra, the process is systematic, and allows reproducible results to be obtained. The patterns observed recur in many different apparent age spectra, so further examination of this phenomenon is necessary. Individual gas reservoirs may correlate with specific features of the microstructure. For example crystal–plastic deformation may introduce defects that vary the length scale for diffusion, and thus influence the effective diffusion radius. Localised deformation may lead to localised recrystallisation, producing new crystalline material with a different microchemistry that will react differently in terms of its retentivity (with respect to solid-state diffusion) or later, in terms of its sensitivity to dehydroxylation, during a step-heating experiment. In this way dehydroxylation may lead to a pattern of gas release that reflects age variation within the microstructure.

The diffusion of argon in muscovite structures needs to be re-examined ab initio, for example using the methods of molecular dynamics, and considering such effects as Penrose tiling on the disorder structure with respect to factors that would determine the rate-determining step for diffusion. In the meantime caution needs to be exerted with respect to the interpretation of apparent age spectra in minerals affected by dehydroxylation in vacuo during step-heating experiments. It is not at all certain that solid state diffusion parallel to the *c*-axis is not the underlying cause of

'stair-case' apparent age spectra in white mica, in which case fossil concentration gradients may be revealed by carefully designed step-heating experiments.

8.6. Effects of excess argon

McDougall and Harrison (1999) correctly note that 'saddle-shaped' shaped spectra (as in Fig. 4) may be the result of excess argon (or data that was not subject to a chlorine correction). On the other hand they also note that "in more modestly affected samples, there are no independent criteria with which to assess whether or not an individual mineral contains (excess argon)". The method of asymptotes and limits makes no assumptions as to process, and thus allows progress. Although we might dismiss an age from a K-feldspar that had yielded a saddled-shaped apparent age spectrum because 'saddle-shaped' spectra had been shown to relate to excess argon, application of the method of asymptotes and limits may reveal correlation of ages obtained with FMAs determined from a collection of minerals over a large dataset. This suggests the FMA reflects an older event, the memory of which is retained within the more retentive domains within the microstructure.

The argon community is perhaps too ready to call on effects related to 'excess argon'. There can be no dispute that excess argon is a factor that needs to be considered in many circumstances. There can also be no argument that many 'problem spectra' are far too readily accorded the benefit of 'excess argon' as a means of explanation for data that do not fit the current geological model. The issue is how to advance beyond this point. FMAs determined by application of the method of asymptotes and limits are by virtue of the technique not at all dependent on "specific knowledge of the underlying system behaviour" (Harrison, pers. comm.). It is precisely this lack of dependence on subjective arguments that provides a distinct advantage for the method of asymptotes and limits. FMAs recognised by virtue of the application of the technique (by definition not possible from a single age spectrum) must then be assessed independently. For example one might not expect 'excess argon' to produce well-defined FMAs, and this raises the possibility that some saddle shaped spectra will allow accurate estimates of the timing of specific geological events.

8.7. Reproducibility and reliability

The method of asymptotes and limits will fail if there is insufficient resolution in the apparent age spectrum. Too few steps in a step-heating schedule (particularly if the initial steps start at too high a temperature) determine a priori that no useful information can ever be extracted by application of the method of asymptotes and limits. In addition the method of asymptotes and limits should be applied to significant datasets, since it is necessary to have sufficient data to determine whether or not the asymptotes and limits cluster with any degree of statistical significance. The principal value of the method of asymptotes and limits lies in the recognition of FMAs that then require separate assessment in order to ascertain their geological significance.

Two significant tests of the method of asymptotes and limits are essential, before it can be fully accepted (Harrison, pers. comm.). One test that is required is that duplicate splits of samples exhibiting complex behaviour should be run and shown to yield a similar distribution of FMAs. The other test that is required is to determine whether particular FMAs on a frequency–magnitude plot have statistical significance. To do this it is necessary to develop a Monte Carlo simulation, and to automate the method of asymptotes and limits. This should allow the determination of whether ideograms similar to those reproduced here can be produced by random processes. In any case caution should be exerted with respect to attributing significance to the FMAs that are defined by relatively low peaks on the frequency–magnitude plots reproduced in this paper.

9. Conclusion

Mixing of argon released from different microstructural gas reservoirs during a step-heating experiment can produce asymptotically converging sequences in measured apparent age spectra. The method of asymptotes and limits focuses on recognising such sequences and by constructing frequency–magnitude plots has the potential to allow recognition of FMAs. In many circumstances individual FMAs can be correlated with specific microstructural reservoirs, allowing constraints to be determined for the age of argon released from these different reservoirs.

In the case that a sequence of apparent ages asymptotically steps towards a limit application of diffusion theory shows that the asymptote provides a bound (either a minimum age or a maximum age depending on the type of asymptote). Analysing the same sequence based on a theory requiring progressive mixing of gas from two microstructural reservoirs can yield the same result. But in either case there is no reason to suspect that an individual asymptote or limit represents a geologically significant 'event'. This view might change if a collection of asymptotes and limits obtained from an extensive dataset produced a set of well-defined FMAs.

The method of asymptotes and limits thus provides an approach to the analysis of data from step heating experiments that is internally consistent and which does not rely upon the subjective determination of what constitutes a 'plateau' in an apparent age spectrum. The technique makes no assumptions as to the processes that occasion the release of argon during a step-heating experiment, and applies equally well to the analysis of

apparent age spectra simulated on the basis that the release mechanism is volumetric diffusion, or to the analysis of apparent age spectra produced from white mica that dehydroxylated during the measurement process.

Acknowledgements

We thank Stan Szczepanski (then at the VIEPS Argon Laboratory at LaTrobe University) for providing technical advice for the analysis of the Otago Schist samples. Prof. Mark Harrison, Dr W.J. Wibrans, Dr A.P. Koppers, Dr David Phillips and Dr R. Norris provided helpful and thorough reviews, numerous discussions, suggestions and encouragement.

References

Baldwin, S.L., 1996. Contrasting P–T–t histories for blueschists from the western Baja Terrane and the Aegean; effects of synsubduction exhumation and backarc extension. In: Bebout, G.E., Scholl, D.W., Kirby, S.H., Platt, J.P. (Eds.), Subduction Top to Bottom. Geophysical Monograph 96, pp. 135–141.

Baldwin, S.L., Lister, G.S., 1998. Thermochronology of the South Cyclades Shear Zone, Ios, Greece—effects of ductile shear in the argon partial retention zone. Journal of Geophysical Research 103, 7315–7336.

Berger, G.W., York, D., 1981. Geothermometry from $^{40}Ar/^{39}Ar$ dating experiments. Geochemica et Cosmochimica Acta 45, 795–811.

Dahl, P.S., 1996. The crystal-chemical basis for argon retention in micas: inferences from interlayer partitioning and implications for geochronology. Contributions to Mineralogy and Petrology 123, 22–39.

Dallmeyer, R.D., Lecorche, J.P., 1990. $^{40}Ar/^{39}Ar$ polyorogenic mineral age record in the northern Mauritanide orogen, West Africa. Tectonophysics 177, 81–107.

Dalrymple, G.B., Lanphere, J.P., 1974. $^{40}Ar/^{39}Ar$ age spectra of some undisturbed terrestial samples. Geochemica et Cosmochimica Acta 38, 715–738.

Dalrymple, G.B., Grommé, C.S., White, R.W., 1975. Potassium–argon age and paleomagnetism of diabase dikes in Liberia: initiation of central Atlantic rifting. Geological Society of America Bulletin 86, 399–411.

Di Vincenzo, G., Ghiribelli, B., Giogetti, G., Palmeri, R., 2001. Evidence of a close link between petrology and isotopic records: constraints from SEM, EMP, TEM and in situ $^{40}Ar–^{39}Ar$ laser analyses on multiple generations of white micas (Lanterman Range, Antarctica). Earth and Planetary Science Letters 192, 389–405.

Fergusson, C.L., Phillips, D., 2001. $^{40}Ar/^{39}Ar$ and K–Ar age constraints on the timing of regional deformation, south coast of New South Wales, Lachlan Fold Belt: problems and implications. Australian Journal of Earth Sciences 48, 395–408.

Fleck, R.J., Sutter, J.F., Elliot, D.H., 1977. Interpretation of discordant $^{40}Ar/^{39}Ar$ age-spectra of mesozoic tholeiites from Antarctica. Geochemica et Cosmochimica Acta 41, 15–32.

Foland, K.A., Gilbert, L.A., Sebring, C.A., Chen, J.F., 1986. $^{40}Ar/^{39}Ar$ ages for plutons of the Monteregian Hills, Quebec: evidence for a single episode of Cretaceous magmatism. Geological Society of America Bulletin 97, 966–974.

Forster, M.A., 2002. Episodicity during orogenesis. PhD thesis. Monash University, Australia.

Forster, M.A., Lister, G.S., 2003. Cretaceous metamorphic core complexes in the Otago Schist, New Zealand. Australian Journal of Earth Sciences 50, 181–198.

Foster, D.A., Gray, D.R., 2000. The structure and evolution of the Lachlan Fold Belt (Orogen) of Eastern Australia. Annual Reviews of Earth and Planetary Science 28, 47–80.

Foster, D.A., Gray, D.R., Kwak, T.A.P., Bucher, M., 1998. Chronology and tectonic framework of turbidite-hosted gold deposits in the Western Lachlan fold belt, Victoria; $^{40}Ar/^{39}Ar$. In: Ramsay, W.R.H., Bierlein, F.P., Arne, D.C. (Eds.), Mesothermal Gold Mineralization in Space and Time. Ore Geology Reviews 13, pp. 229–250.

Gillespie, A.R., Huneke, J.C., Wasserburg, G.J., 1982. An assessment of $^{40}Ar–^{39}Ar$ dating of incompletely degassed xenoliths. Journal of Geophysical Research 87, 9247–9257.

Hames, W.E., Bowring, S.A., 1994. An empirical evaluation of the argon diffusion geometry in muscovite. Earth and Planetary Science Letters 124, 161–167.

Hames, W.E., Cheney, J.T., 1997. On the loss of $^{40}Ar^{*}$ from muscovite during polymetamorphism. Geochimica et Cosmochimica Acta 61, 3863–3872.

Harrison, T.M., Wang, S., 1981. Further $^{40}Ar/^{39}Ar$ evidence for the multi-collisional heating of the Kirin meteorite. Geochimica et Cosmochimica Acta 45, 2513–2517.

Harrison, T.M., Heizler, M.T., Lovera, O.M., 1993. In vacuo crushing experiments and K-feldspar thermochronometry. Earth and Planetary Science Letters 117, 169–180.

Heizler, M.T., Ralser, S., Karlstrom, K.E., 1997. Late proterozoic (Grenville?) deformation in central New Mexico determined from single-crystal muscovite $^{40}Ar/^{39}Ar$ spectra. Precambrian Research 84, 1–15.

Hodges, K.V., Hames, W.E., Bowring, S.A., 1994. $^{40}Ar/^{39}Ar$ age gradients in micas from a high temperature–low pressure metamorphic terrain. Evidence for very slow cooling and implications for the interpretations of age spectra. Geology 22, 55–58.

Horn, P., Jessberger, E.K., Kirsten, T., Richter, H., 1975. $^{39}Ar–^{40}Ar$ dating of lunar rocks: effects of grain size and neutron irradiation. Geochimica et Cosmochimica Acta (Proceedings of Sixth Lunar Science Conference) Supplement 6, 1563–1591.

Huneke, J.C., Smith, S.P., 1976. The realities of recoil: ^{39}Ar recoil out of small grains and anomalous patterns in $^{39}Ar–^{40}Ar$ dating. Geochimica et Cosmochimica Acta (Proceedings of the Seventh Lunar Science Conference) Supplement 7, 1987–2008.

Koppers, A.A.P., Staudigel, H., Wijbrans, J.R., 2000. Dating crystalline groundmass separates of altered cretaceous seamount basalts by the $^{40}Ar/^{39}Ar$ incremental heating technique. Chemical Geology 166, 139–158.

Lanphere, M.A., Dalrymple, G.B., 1971. A test of the $^{40}Ar/^{39}Ar$ spectrum technique on some terrestrial materials. Earth and Planetary Science Letters 12, 359–372.

Lanphere, M.A., Dalrymple, G.B., 1976. Identification of excess ^{40}Ar by the $^{40}Ar/^{39}Ar$ age spectrum technique. Earth and Planetary Science Letters 32, 141–148.

Lister, G.S., Baldwin, S.L., 1996. Modelling the effect of arbitrary P–T–t histories on argon diffusion in minerals using the MacArgon program for Apple Macintosh. Tectonophysics 253, 83–109.

Lister, G.S., Snoke, A.W., 1984. S–C mylonites. Journal of Structural Geology 6, 617–638.

Lovera, O.M., Grove, M., Harrison, T.M., 1989. The $^{40}Ar/^{39}Ar$ geothermometry for slowly cooled samples having a distribution of diffusion domain sizes. Journal of Geophysical Research 94, 17917–17935.

McDougall, I., Harrison, T.M., 1999. Geochronology and Thermochronology by the $^{40}Ar/^{39}Ar$ Method. Oxford University Press, Oxford.

Pankhurst, R.J., Moorbath, S., Rex, D.C., Turner, G., 1973. Mineral age patterns in ca. 3700 MY old rocks from West Greenland. Earth and Planetary Science Letters 20, 157–170.

Robbins, G.A., 1972. Radiogenic argon diffusion in muscovite under hydrothermal conditions. M.Sc. thesis, Brown University.

Scaillet, S., Féraud, G., Ballèvre, M., Amouric, M., 1992. Mg/Fe and (Mg, Fe)$Si–Al_2$ compositional control on argon behaviour in high-pressure white micas: a $^{40}Ar/^{39}Ar$ continuous laser-probe study from

the Dora–Maira nappe of the internal western Alps, Italy. Geochimica et Cosmochimica Acta 56, 2851–2872.

Sletten, V.W., Onstott, T.C., 1998. The effect of the instability of muscovite during in vacuo heating on $^{40}Ar/^{39}Ar$ step-heating spectra. Geochimica et Cosmochimica Acta 62, 123–141.

Snee, L.W., Sutter, J.F., Kelly, W.C., 1988. Thermochronology of economic mineral deposits: dating the stages of mineralization at Panaqueira, Portugal, by high precision $^{40}Ar/^{39}Ar$ age spectrum techniques on muscovite. Economic Geology 83, 335–354.

Turner, G., 1968. The distribution of potassium and argon in chondrites. In: Ahrens, L.H. (Ed.), Origin and Distribution of the Elements. Pergamon, London, pp 387–398.

Turner, G., Miller, J.A., Grasty, R.L., 1966. The thermal history of the Bruderheim meteorite. Earth and Planetary Science Letters 1, 155–157.

Urai, J.L., Means, W.D., Lister, G.S., 1989. Dynamic recrystallisation of minerals. In: Hobbs, B.E., Heard, H.C. (Eds.), Mineral and Rock Deformation: Laboratory Studies—the Paterson Volume. American Geophysical Union, Geophysical Monograph 16, pp. 161–199.

Villa, I.M., 1998. Isotopic closure. Terra Nova 10, 42–47.

Wang, S., McDougall, I., Tetley, N., Harrison, T.M., 1980. $^{40}Ar/^{39}Ar$ age and thermal history of the Kirin chondrite. Earth and Planetary Science Letters 49, 117–131.

Wijbrans, J.R., McDougall, I., 1986. $^{40}Ar/^{39}Ar$ dating of white micas from an Alpine high pressure metamorphic belt on Naxos (Greece): the resetting of the argon isotopic system. Contributions to Mineralogy and Petrology 93, 187–194.

Wijbrans, J.R., McDougall, I., 1988. Metamorphic evolution of the Attic Cycladic metamorphic belt on Naxos (Cyclades, Greece) utilising $^{40}Ar/^{39}Ar$ age spectrum measurements. Journal of Metamorphic Geology 6, 571–594.

Wijbrans, J.R., Pringle, M.S., Koppers, A.A.P., Scheveers, R., 1995. Argon geochronology of small samples using the Vulkaan argon laserprobe. Proceedings Koninklijke Nederlandse Akademie van Wetenschappen 98 (2), 185–218.

Zeitler, P.K., 1987. Argon diffusion in partially out-gassed alkali feldspars: Insights from $^{40}Ar/^{39}Ar$ analysis. Chemical Geology (Isotope Geoscience Section) 65, 167–181.